JOURNAL OF MATERIALS SCIENCE 27 (1992) 947–955

Chord intercepts in a two-dimensional cell growth model

Part III *Chord intercepts in an experiment*

G. E. W. SCHULZE, W. A. SCHULZE
Abteilung Werkstoffwissenschaft (IPkM), Heinrich-Heine-Universität Düsseldorf, Düsseldorf D-4000 Düsseldorf, Germany

A foil of polypropylene is heat-treated in such a manner that a "growing 2D cell-model" is formed. A Rosiwal's line is placed into the totally primarily crystallized foil. The nucleus-coordinates of grains intercepting Rosiwal's line are measured. From these "effective" nuclei we determine at fraction transformed $F = 1/4$, $1/2$ and $3/4$ the distributions of grain-lengths and melt-lengths. Further we determine properties which are derived from the chord intercepts at a given F. Experimentally we find that the values (Poisson distribution of nuclei, chord intercepts, etc.) are in good agreement with the growing 2D cell-model.

1. Introduction

In Part I [1] of the present series we defined a "growing 2D cell-model at fraction transformed, F" and its Rosiwal's line. In Part I [1] and Part II [2] we calculated along Rosiwal's line at a given F the theoretical distribution densities (or "relative frequencies") of the melt-lengths and grain-lengths of type 1, 2 and 3. A grain-length of type 1 borders on melt-intervals, type 3 borders on neighbouring grain-lengths, and type 2 borders on a melt-interval and a grain-length.

The present paper deals with an indirect experimental measurement of melt-lengths and grain-lengths at $F = 1/4$, $1/2$, $3/4$ and 1 and with the results obtained. These are compared with the theoretical results, and good agreement is obtained.

The paper is organized as follows. In Section 2 a foil of polypropylene is described which is heat-treated in such a manner that the conditions of the "growing 2D cell-model" are nearly fulfilled. In Section 3 this is proved. In Section 4 we measure all nucleus-coordinates of grains intercepting Rosiwal's line at $F = 1$. Out of these "effective" nuclei we determine those grains which reach Rosiwal's line at $F = 1/4$, $1/2$ and $3/4$, and we calculate the lengths along Rosiwal's line of the melt-intervals and the grains of type 1, 2 and 3. Section 5 deals with the properties thus derived and their dependence on F through the mean length of melt-intervals, $\bar{a}(F)$. In Section 6 a computer simulation is executed with only some thousands of effective nuclei. This gives an estimation of statistical fluctuations. Section 7 discusses the tests in Sections 4 and 5 and shows that the values (Poisson distribution of nuclei, chord intercepts, etc.) in the experiment are in good agreement with the growing 2D cell-model.

2. Production of sample

We used a foil of isotactic polypropylene (Hoechst AG) with a thickness of 4 μm and dimensions of 40 mm × 20 mm. It had an isotacticity of 96% and $M_W = 300\,000$. Stabilizers are not used in the product.

We covered a glass slide, 75 mm × 25 mm × 1 mm, with the foil which was fastened point by point with the gum "Uhu plus schnellfest". For temperature-symmetry the foil was covered with a second slide in order to produce a sandwich. This sandwich was put into a Mettler microscope heat-stage FP 52 with the steering gear FP 5 in order to obtain a uniform and adjustable temperature for the whole sample.

Fig. 1 shows the heat-treatment of the foil. By raising the temperature to 230 °C and dropping it to 140 °C the melted foil is transferred into a supercooled state because its melting point is 169 °C. Then we change temperature to 126.5 °C for 1 min, where nuclei are formed. We further raise the temperature to 153 °C, when the nuclei of the desired α-modification are preserved but the nuclei of the unwanted β-modification disappear. On changing the temperature to 133 °C, grains grow out of the α-nuclei. In order to set marks of the growth-fronts [3], we raise the temperature to 144 °C so that the growthrate of the marks amounts to 1/10 of the normal growth-rate at 133 °C. This procedure is repeated. Fig. 2 shows the microstructure at 20 °C with marks produced by the heat-treatment of Fig. 1.

3. Test of Poisson distribution of the nuclei

Fig. 2 shows that all grains start simultaneously to grow. The grains grow circularly with the same constant growth-rate. The latter follows from the equidistant marks which are set at equidistant points of time. If two grains touch they form a straight grain boundary. At last there are polygons of grain boundaries forming the grains.

0022–2461

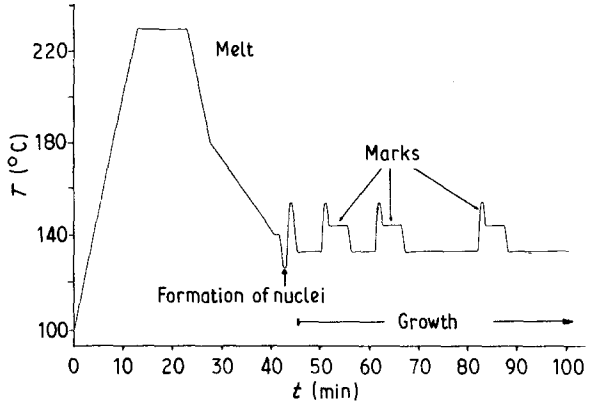

Figure 1 Heat-treatment programme of the foil.

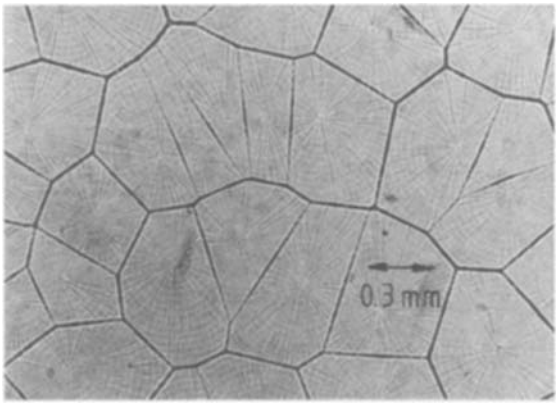

Figure 2 Microstructure with marks, obtained after finished heat-treatment programme of Fig. 1.

These are the conditions of the "growing 2D cell-model" except one: the centres of grains (nuclei) are Poisson-distributed within the foil. To show this we need the whole area of the sample (35 mm × 20 mm). We place a test-area with dimensions of 0.69 mm × 0.98 mm into the sample area. The test-area contains a mean of 4.32 nuclei. A screening process with the test-area shows how many times we find 0, 1, 2, 3, . . . nuclei within the test-area. The result is shown in Fig. 3. In Fig. 3 the dashed lines represent a Poisson distribution with $\bar{n} = 4.32$ nuclei per test-area:

$$p_k(\bar{n}) = \frac{\bar{n}^k}{k!}\exp(-\bar{n})$$

The χ^2-test gives a significance level of 10%.

We remark that in future we choose a "length unit" (l.u.) in such a manner that per (length unit)^2 there is on average one nucleus:

$$1\ \text{l.u.} = \frac{1}{(\text{mean number of nuclei per mm}^2)^{1/2}}$$

Because the mean density of nuclei amounts to 6.38 nuclei per mm^2, 1 l.u. $\simeq$ 0.396 mm.

4. Tests of chord intercepts at $F = 1$ and at $F = 0.25; 0.5; 0.75$

After the heat-treatment (Fig. 1) is finished, we regard

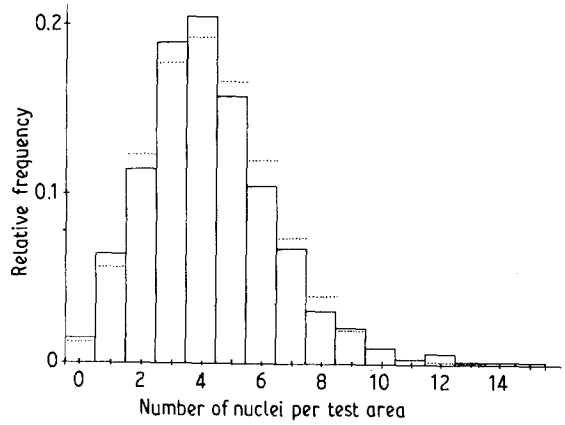

Figure 3 Poisson distribution and experimental relative frequency with $\bar{n} = 4.32$ nuclei per test area.

the whole area of 35 mm × 20 mm in the state which is obtained at a temperature of 20 °C. In this crystallized state we put in the length direction 16 parallel lines with a separation of about 1 mm. The 16 lines are combined to one Rosiwal line with total length of 3422 length units. The combination of the lines is arranged in such a way that the last nucleus of line i has the same y-value (perpendicular distance) as the first nucleus of line $(i + 1)$ with $i = 1, 2, 3, \ldots 15$. We determine the chord intercepts at $F = 1$ as 4226. From these 4226 grains intercepting Rosiwal's line, we measure the coordinates (x, y) of their nuclei. Thereby the x-axis is identified with Rosiwal's line and the y-values are the perpendicular distances of nuclei from Rosiwal's line.

Then we calculate for all nuclei which reach Rosiwal's line at $F = 0.25$, 0.5 and 0.75, using the experimentally measured coordinates of the 4226 nuclei at $F = 1$. Hence we determine their grain-lengths and their melt-lengths. Fig. 4 indicates the relative frequency $A'(a, F)$ of melt-interval lengths a at $F = 0.25$, 0.5 and 0.75. The step diagram gives an account of experimental values and the dashed curve illustrates the theoretical distribution density.

Figs 5, 6 and 7 show the relative frequencies, $B'(b, F)$, of grain-lengths b at $F = 0.25$, 0.5 and 0.75. In Figs 5a, 6a and 7a all grain-lengths b are represented. In Figs 5b–d, 6b–d and 7b–d the fractions of grain-lengths of type 1, 2 and 3 are specified, respectively.

5. Tests of quantities derived from F and R

The radius of all growing grains (R in length units) effects a fraction transformed, F. This F is the sum of all grain-lengths along Rosiwal's line at R, divided by the whole length of Rosiwal's line. But the measurement of grain lengths is inexact. For that reason the $F(R)$ is determined by measurement of the perpendicular distance of effective nuclei at R and by calculation of the sum of coordinated grain-lengths, divided by the length of Rosiwal's line.

$F_{\text{theory}}(R)$ of the growing 2D cell-model amounts to $F_{\text{theory}}(R) = 1 - \exp(-\pi R^2)$. Fig. 8b shows $F_{\text{exp}}(R)$

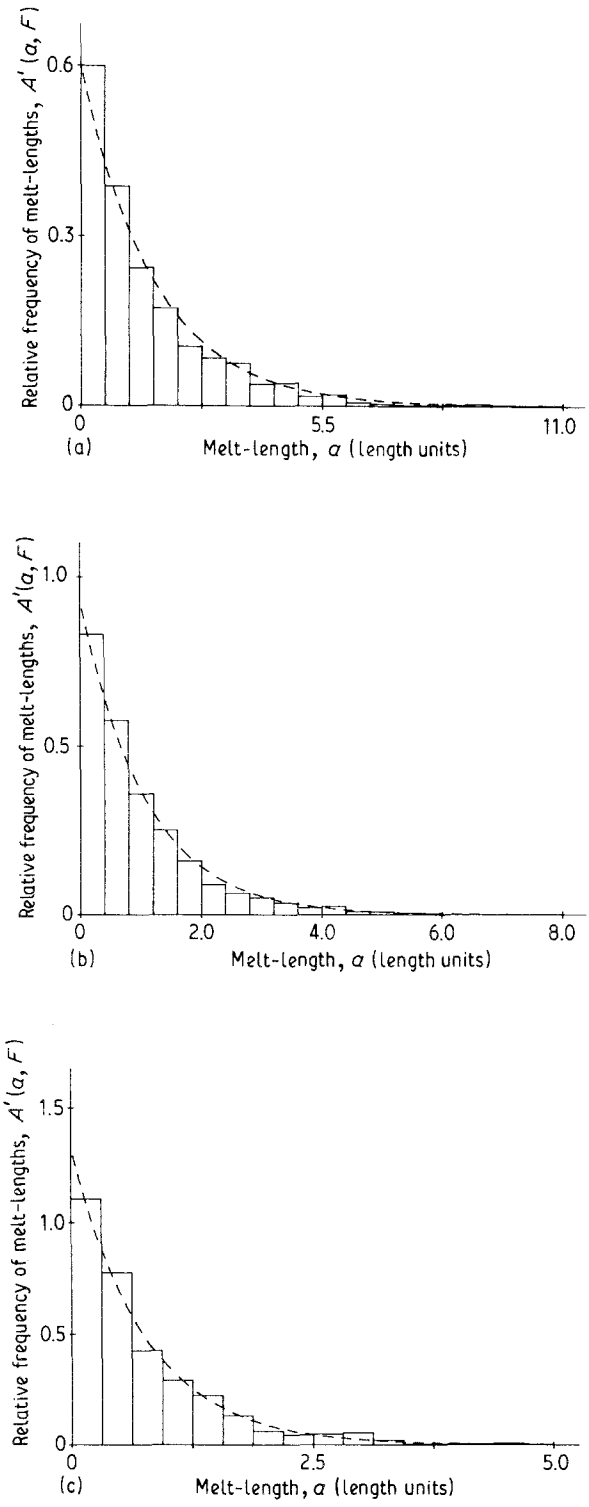

Figure 4 Relative frequencies of melt-lengths at (a) $F = 1/4$ ($N_A = 1349$), (b) $F = 1/2$ ($N_A = 1606$), (c) $F = 3/4$ ($N_A = 703$).

(solid line) and $F_{\text{theory}}(R)$ (dashed). Besides R we also use F_{theory} as an independent variable. This is shown in Fig. 8a, where F_{theory} and F_{exp} are represented in dependence on F_{theory}.

The following quantities are represented by F as well as by R:

1. F_1, F_2, F_3 are respectively the fractions transformed of type 1, 2, 3. They are represented in Fig. 9.

2. $D_i = F_i/F$ is the fraction transformed for type i which is divided by F, as shown in Fig. 10.

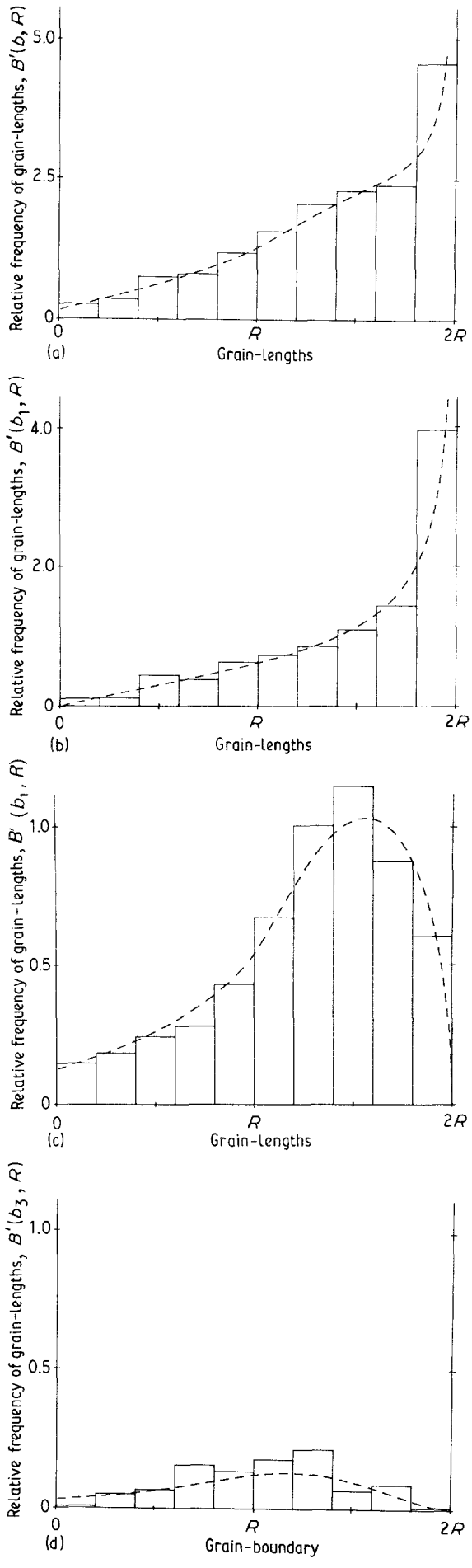

Figure 5 Relative frequency of grain-lengths at $F = 1/4$, $R = 0.303$ l.u.: (a) all grains included ($N_A = 2195$), (b) fraction of type 1 ($N_A = 1315$), (c) fraction of type 2 ($N_A = 749$), (d) fraction of type 3 ($N_A = 131$).

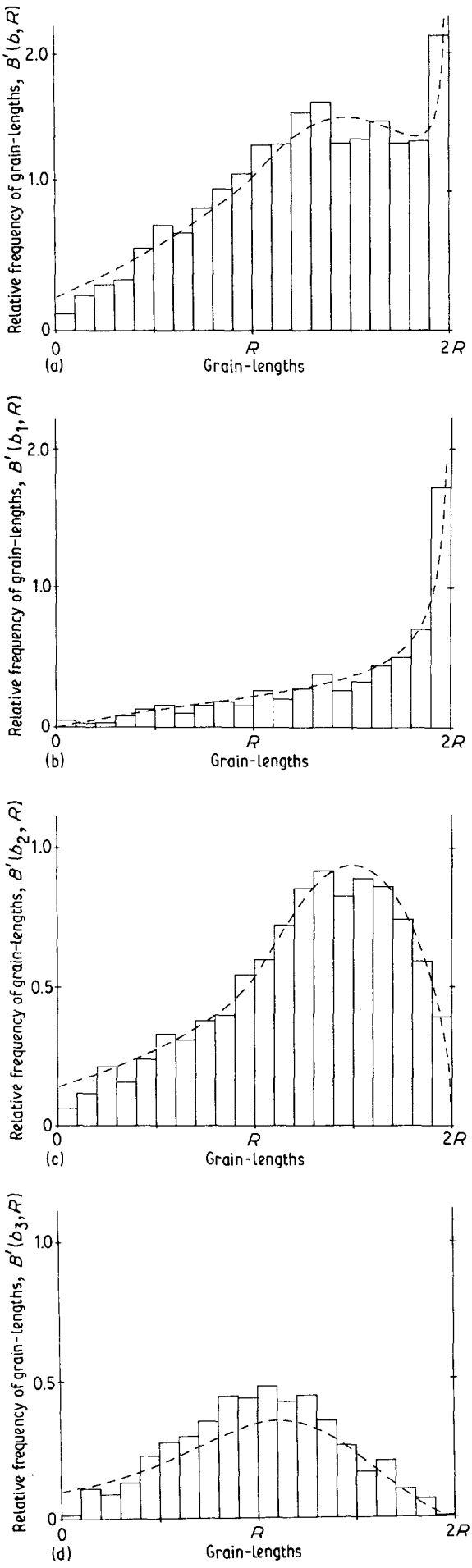

Figure 6 Relative frequency of grain-lengths at $F = 1/2$, $R = 0.470$ l.u.: (a) all grains included ($N_A = 3088$), (b) fraction of type 1 ($N_A = 904$), (c) fraction of type 2 ($N_A = 1475$), (d) fraction of type 3 ($N_A = 709$).

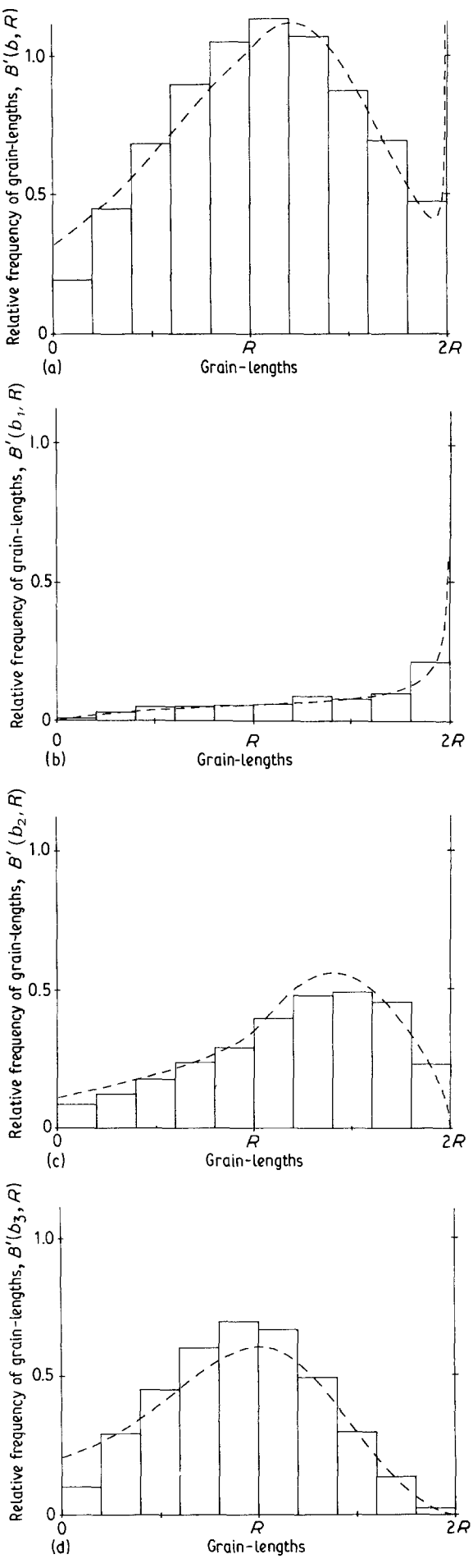

Figure 7 Relative frequency of grain-lengths at $F = 3/4$, $R = 0.664$ l.u.: (a) all grains included ($N_A = 3731$), (b) fraction of type 1 ($N_A = 370$), (c) fraction of type 2 ($N_A = 1481$), (d) fraction of type 3 ($N_A = 1880$).

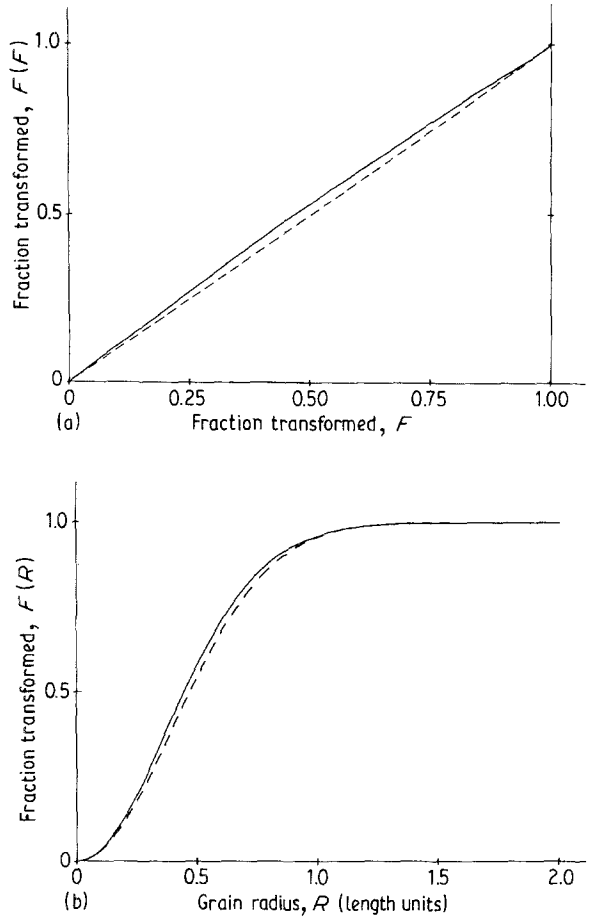

Figure 8 (– – –) F_{theory} and (——) F_{exp} in dependence on (a) F_{theory} and (b) grain radius R.

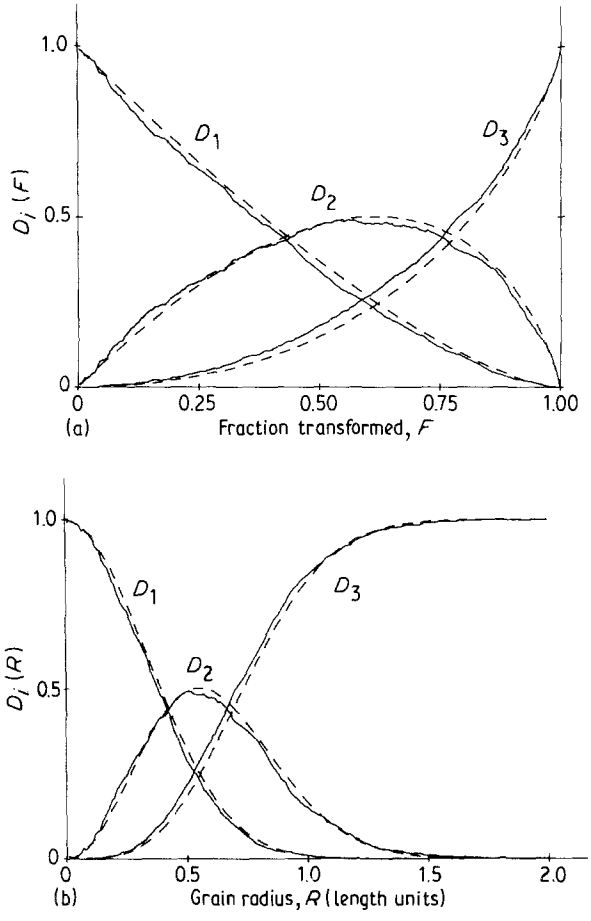

Figure 10 $D_i = F_i/F$ in dependence on (a) F_{theory} and (b) R.

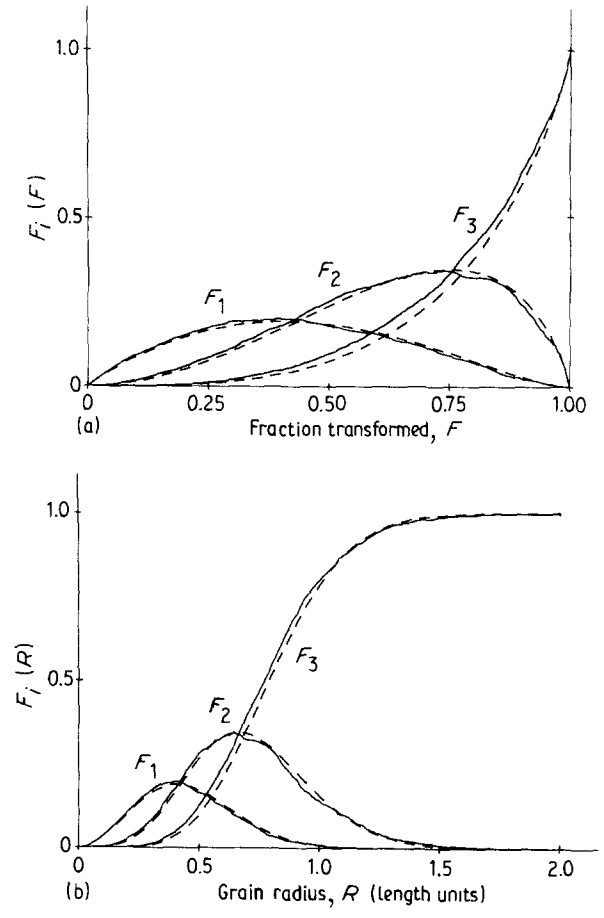

Figure 9 F_1, F_2 and F_3 in dependence on (a) F_{theory} and (b) grain radius R.

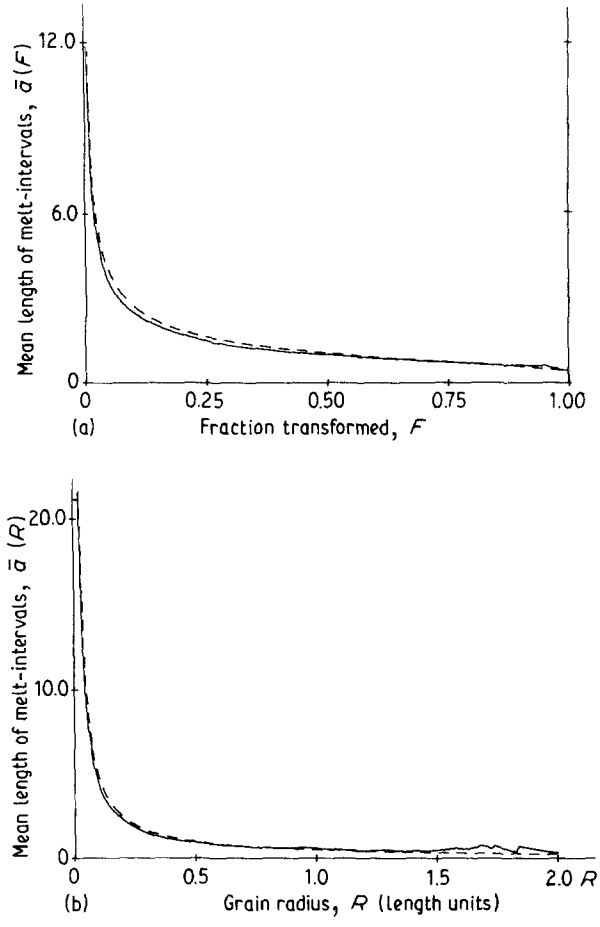

Figure 11 Mean length of melt intervals in dependence on (a) F_{theory} and (b) R.

3. The mean length of melt-intervals is represented in Fig. 11.

4. The mean length of grain-lengths is represented in Fig. 12.

5. N_1, N_2, N_3 and $N_{\text{eff}} = N_1 + N_2 + N_3$ are the number of coordinated grain-types per length unit on Rosiwal's line. Results are represented in Fig. 13.

6. $W_i = N_i/N_{\text{eff}}$ can be obtained as a number of grains of type i, divided by all grains along Rosiwal's line (Fig. 14).

7. N_{move} (all moved borders of the spherulites on Rosiwal's line), N_{fix} (all fixed grain boundaries on Rosiwal's line) and $N_{\text{total}} = N_{\text{move}} + N_{\text{fix}}$ per length unit are presented in Fig. 15.

6. Simulation of tests

A computer simulation of the growing 2D cell-model leads in practice to the theoretical curves, if we take 10^7–10^9 effective values (nuclei, chord intercepts etc.). Simulating only about 5×10^3 values – conforming to the number of experimental values – the curve shows statistical fluctuations in comparison with the theoretical curve.

In Figs 16 to 25 we show the influence of statistical fluctuations, in which the theoretical curve is dashed and the simulated curve is a solid line. The number of values is noted in the captions. We used some selected tests from Sections 4 and 5.

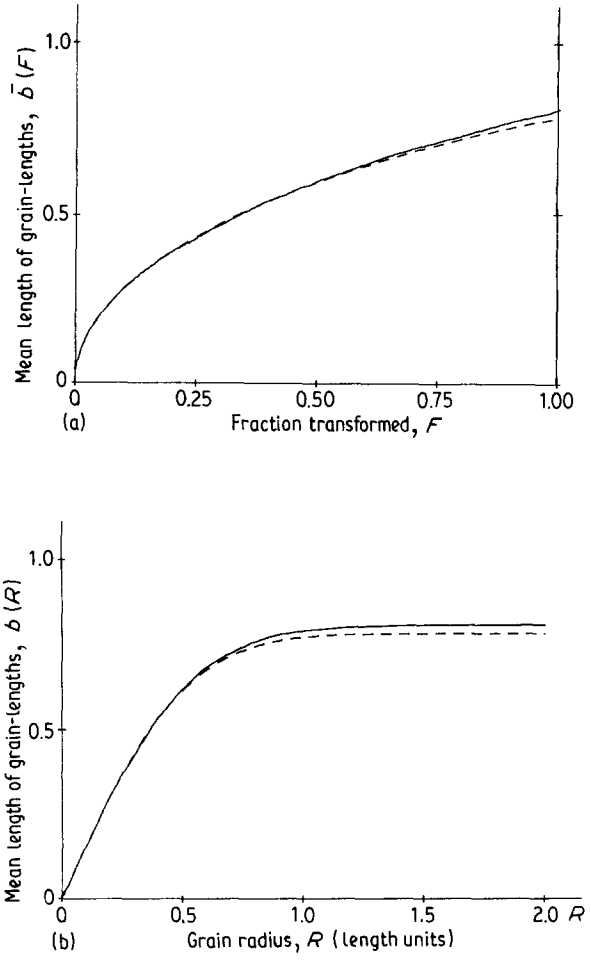

Figure 12 Mean grain-lengths in dependence on (a) F_{theory} and (b) R.

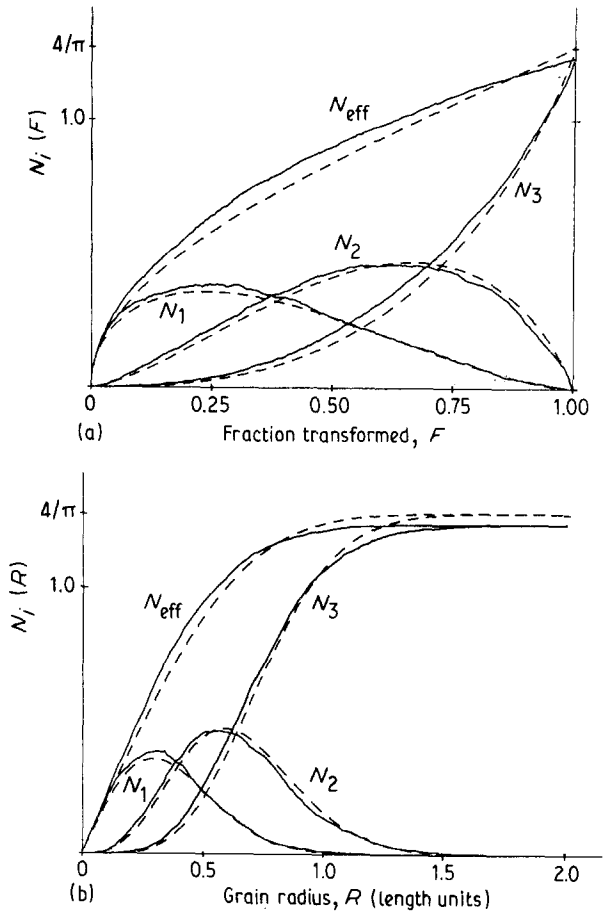

Figure 13 Number per length unit N_1, N_2, N_3 and $N_{\text{eff}} = N_1 + N_2 + N_3$ in dependence on (a) F_{theory} and (b) R.

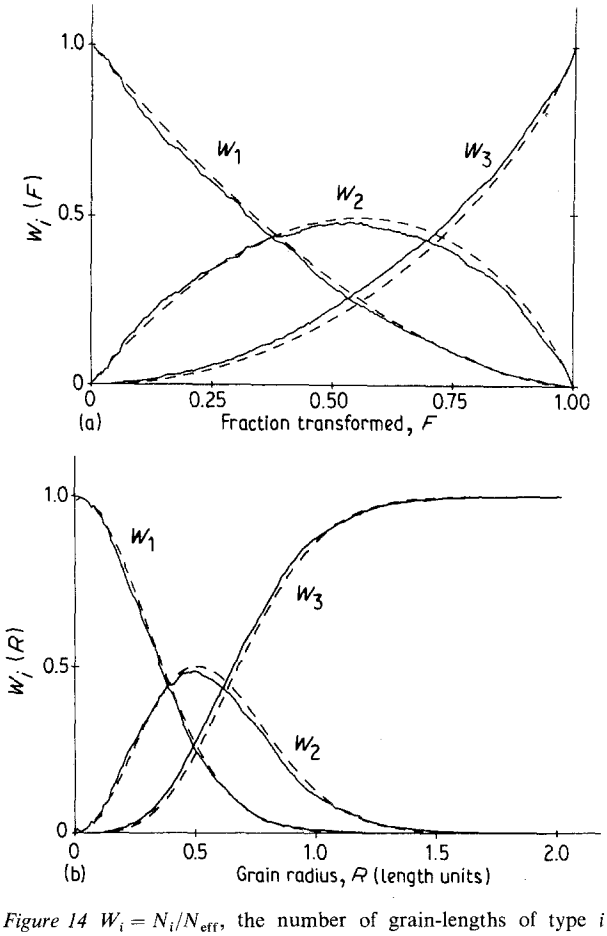

Figure 14 $W_i = N_i/N_{\text{eff}}$, the number of grain-lengths of type i divided by the number of all grain-lengths, in dependence on (a) F_{theory} and (b) R.

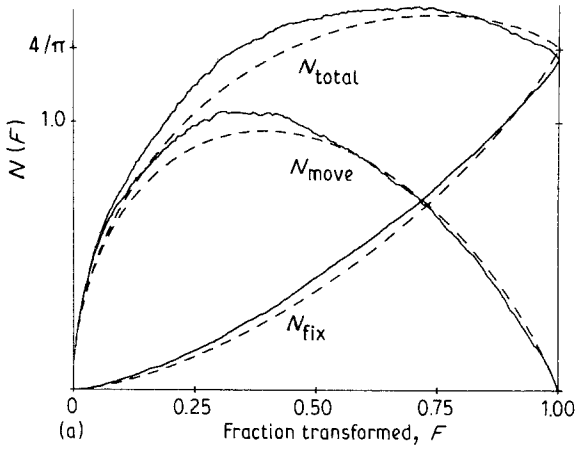

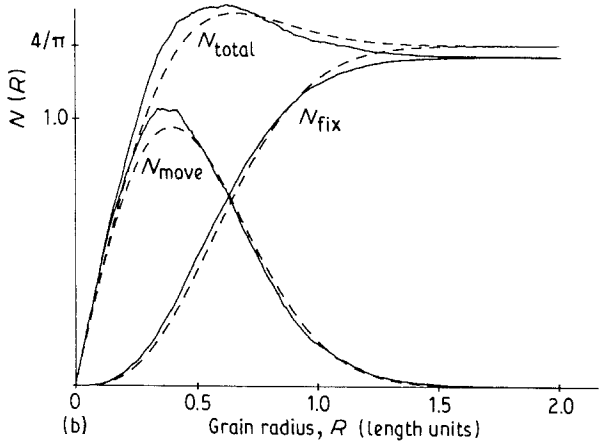

Figure 15 N_{move}, N_{fix} and N_{total}, all moved and fixed borders per length unit, in dependence on (a) F_{theory} and (b) R.

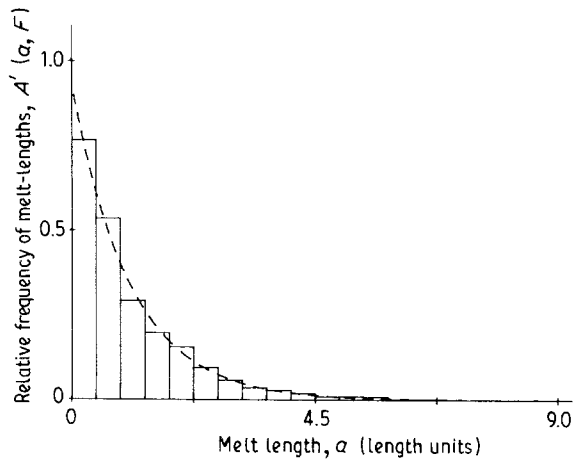

Figure 16 Relative frequencies of melt-lengths at $F = 1/2$: (——) curve of simulation, (– – –) theoretical curve ($N_A = 1858$).

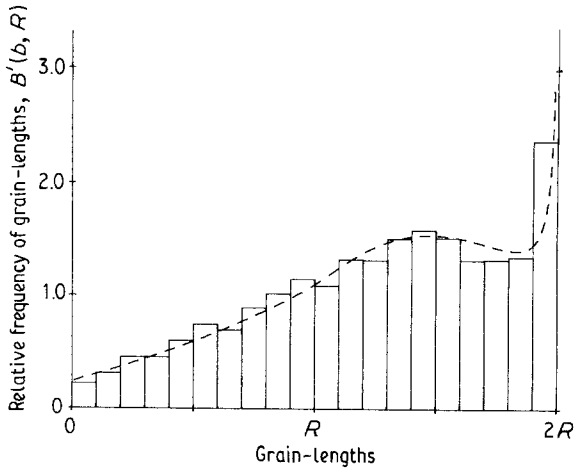

Figure 17 Relative frequency of grain-lengths at $F = 1/2$ where all grains are included: (——) curve of simulation, (– – –) theoretical curve ($R = 0.470$ l.u., $N_A = 3354$).

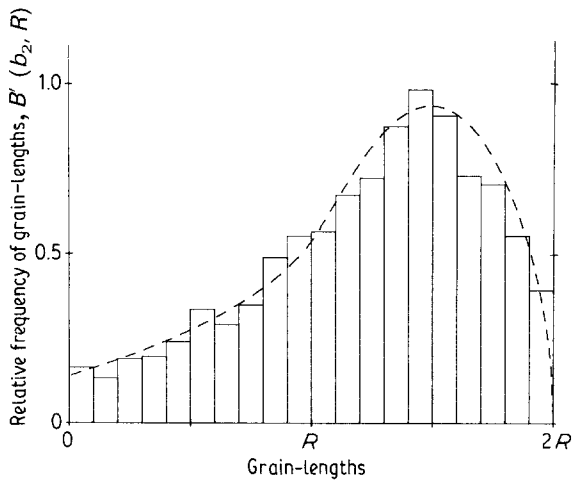

Figure 18 Relative frequency of grain-lengths at $F = 1/2$ where fraction of type 2 is determined: (——) curve of simulation, (– – –) theoretical curve. ($R = 0.470$ l.u., $N_A = 1584$).

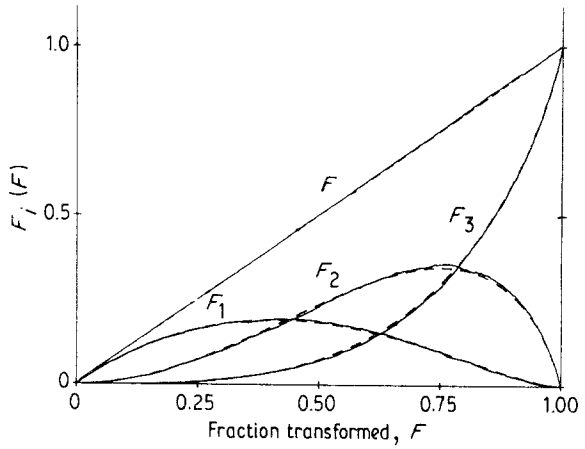

Figure 19 (– – –) F_{theory} and (——) simulated curve of F with 5000 values, in dependence on (a) F_{theory} and (b) grain radius R.

7. Discussion of tests

The following assumptions of the growing 2D cell-model are fulfilled in theory, in simulation and in experiment: all grains start to grow simultaneously and grow circularly with the same constant growth-rate. If two grains touch, their growth is finished there.

The additional postulate, that we have an infinity of nuclei which are Poisson-distributed, is distinguished by three cases. In the theoretical case the postulate is completely fulfilled. In the case of simulation the nuclei are Poisson-distributed, but for some thousands of nuclei statistical fluctuations are present. In the experimental case we take into consideration some

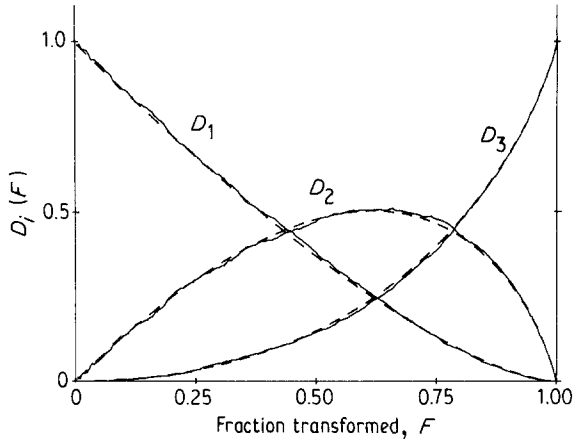

Figure 20 (——) Simulated curve of D_i with 5000 values, and (– – –) theoretical curve in dependence on F_{theory}.

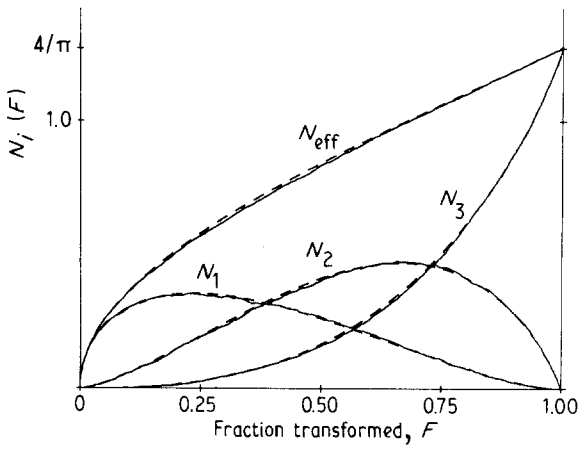

Figure 23 (——) Simulated curve of N_1, N_2, N_3 and N_{eff} with 5000 values, and (– – –) theoretical curve in dependence on F_{theory}.

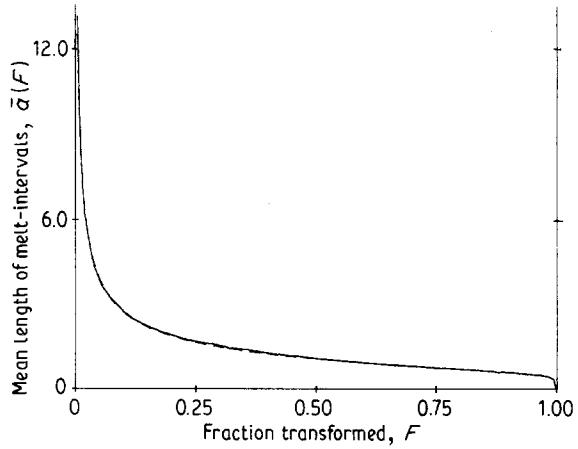

Figure 21 (——) Simulated curve of mean length of melt-intervals with 5000 values, and (– – –) theoretical curve in dependence on F_{theory}.

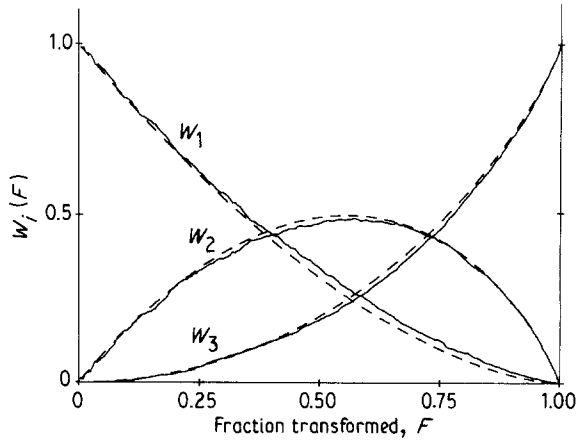

Figure 24 (——) Simulated curve of $W_i = N_i/N_{\text{eff}}$ with 5000 values, and (– – –) theoretical curve in dependence on F_{theory}.

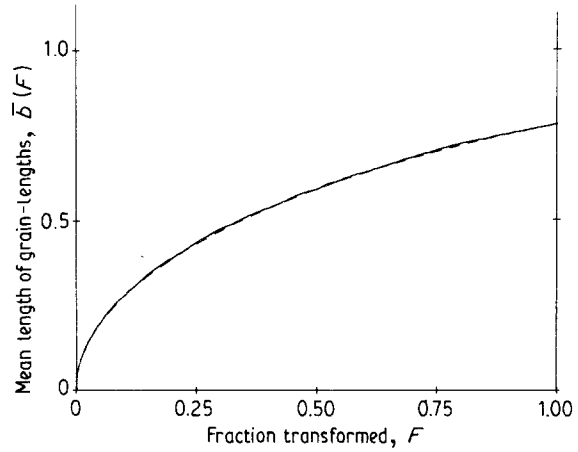

Figure 22 (——) Simulated curve of mean length of grain-lengths with 5000 values, and (– – –) theoretical curve in dependence on F_{theory}.

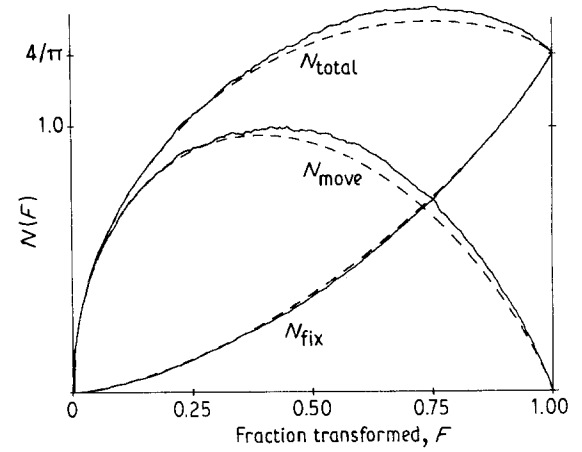

Figure 25 (——) Simulated curve of N_{move}, N_{fix} and N_{total} with 5000 values, and (– – –) theoretical curve in dependence on F_{theory}.

thousands of nuclei with errors of measurement. Therefore experimental curves will deviate more from the theoretical curves than simulated curves.

The Poisson distribution of nuclei in the experimental case was examined by use of a χ^2-test. A significance level of 10% normally represents a distribution close to a Poisson distribution, but there is no criterion for whether a significance level of 10% is sufficient for this kind of analysis. Only a comparison with curves of the three cases can answer the question:

are the results of tests from Sections 4 and 5 in good or in bad agreement? Looking at the tests, we think that the experimental values (nuclei, chord intercepts etc.) are a good approximation to the growing 2D cell-model.

References

1. G. E. W. SCHULZE and H.-P. WILBERT, *J. Mater. Sci.* **24** (1989) 3101.
2. G. E. W. SCHULZE, L. O. SCHWAN and R. WILLERS, *ibid.* **24** (1989) 3107.
3. G. E. W. SCHULZE and H.-P. WILBERT, *J. Mater. Sci. Lett.* **8** (1989) 71.

Received 11 October 1990
and accepted 1 May 1991